Inorganic Chemistry
Article
pubs.acs.org/IC

Structure and Thermodynamic Properties of $(C_5H_{12}N)CuBr_3$: A New Weakly Coupled Antiferromagnetic Spin-1/2 Chain Complex Lying in the 1D–3D Dimensional Cross-Over Regime

Bingying Pan,[†,‡] Yang Wang,[†] Lijuan Zhang,*[,†] and Shiyan Li*[,†,‡]

[†]Laboratory of Advanced Materials, Fudan University, Shanghai 200438, P. R. China
[‡]State Key Laboratory of Surface Physics, Department of Physics, Fudan University, Shanghai 200433, P. R. China

Supporting Information

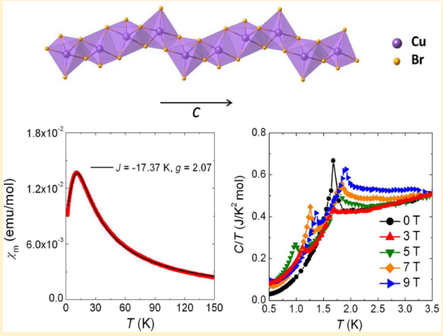

ABSTRACT: Single crystals of a metal organic complex $(C_5H_{12}N)CuBr_3$ ($C_5H_{12}N$ = piperidinium, pipH for short) have been synthesized, and the structure was determined by single-crystal X-ray diffraction. $(pipH)CuBr_3$ crystallizes in the monoclinic group $C2/c$. Edging-sharing $CuBr_5$ units link to form zigzag chains along the c axis, and the neighboring Cu(II) ions with spin-1/2 are bridged by bibromide ions. Magnetic susceptibility data down to 1.8 K can be well fitted by the Bonner–Fisher formula for the antiferromagnetic spin-1/2 chain, giving the intrachain magnetic coupling constant $J \approx -17$ K. At zero field, $(pipH)CuBr_3$ shows three-dimensional (3D) order below T_N = 1.68 K. Calculated by the mean-field theory, the interchain coupling constant J' = −0.91 K is obtained and the ordered magnetic moment m_0 is about 0.23 μ_B. This value of m_0 makes $(pipH)CuBr_3$ a rare compound suitable to study the 1D–3D dimensional cross-over problem in magnetism, since both 3D order and one-dimensional (1D) quantum fluctuations are prominent. In addition, specific heat measurements reveal two successive magnetic transitions with lowering temperature when external field $\mu_0H \geq 3$ T is applied along the a' axis. The μ_0H-T phase diagram of $(pipH)CuBr_3$ is roughly constructed.

■ INTRODUCTION

Conventional 3D magnets are described by the semiclassical spin wave theory, whereas 1D magnets are described fully by quantum theory.[1] Of particular interest is the Heisenberg antiferromagnetic (HAFM) spin chain, which represents one of the few exactly solvable many-body models in quantum physics.[2,3] The HAFM spin chain is a disordered system, which means that the system does not show any magnetic order even at absolute zero temperature.[2,3] It has fractional excitations called spinons.[4] The multispinon continuum spectrum is distinct from the sharp spin wave spectrum in conventional 3D magnets.[4] In real compounds, the weak interchain interaction J' between HAFM spin chains will lead the system to a 3D ordered state at sufficiently low temperature. Such a 3D ordered state is essentially different from that of conventional 3D magnets, since its spectrum has both sharp spin waves at low energies and multispinon continuum at high energies.[5−10] In this sense, the 3D ordered state of weakly coupled HAFM spin chains lies in the cross-over regime from quantum to semiclassical physics. A novel longitudinal spin wave mode, which does not exist in conventional 3D magnets, is predicted to emerge by mean-field and random phase approximation theories (MF/RPA).[11,12] However, the results of inelastic neutron scattering experiments showed substantial discrepancies with theories, which was attributed to the ignorance of correlation effects in MF/RPA.[9,10,13,14] Therefore, the 1D–3D dimensional cross-over problem remains to be solved in magnetism, although a large amount of information is already available on these systems.[7,9,14,15]

The real compounds of weakly coupled HAFM spin chains can be classified into two categories. The first one is copper(II)-based inorganic compounds such as $BaCu_2Si_2O_7$,[16] $SrCuO_2$ and Sr_2CuO_3,[17] Ca_2CuO_3,[18] and $KCuF_3$,[19] in which J is on the order of −1000 K. The second one is 1D molecular magnets in which $-J$ is usually below 100 K.[20] The 1D molecular magnets are mostly metal–organic complexes such as copper benzoate,[21] copper pyrimidine,[22,23] copper pyrazine dinitrate,[24] and $CuCl_2{\cdot}2((CH_3)_2SO)$,[25] in which the spins of neighboring Cu(II) ions interact via water molecules, halide ions, or bridging ligands.[20] The ordered state of weakly coupled HAFM spin chains has a dual 1D and 3D character, which means that 3D magnetic order and 1D quantum fluctuations coexist in the system.[8,11] The ordered static magnetic moment m_0 is used as a criterion to evaluate whether the system is more 1D or 3D like.[15] The m_0 stems from the unpaired electrons in the outer shell of a magnetic ion. Since the Cu(II) ion has one unpaired d electron, its m_0 should be 1 Bohr magneton, μ_B. However, in the ordered state of a copper-based weakly coupled chain

Received: December 19, 2013
Published: March 11, 2014

dx.doi.org/10.1021/ic403100h | Inorg. Chem. 2014, 53, 3606−3610

system, only a fraction of the spin moment becomes static.[15,25−27] In this situation, m_0 has a finite value smaller than 1 μ_B. A system suitable to study the 1D−3D dimensional cross-over problem should have a proper value of m_0, so that both the 1D and the 3D character are prominent. However, real compounds that meet this condition are rare. To our knowledge, $BaCu_2Si_2O_7$ with $m_0 = 0.16\ \mu_B$ is one suitable compound,[8,9,14,15,28] while the m_0 of other compounds is either too small or too large.[15,25−27] Due to the lack of satisfactory theory of the 1D−3D dimensional cross-over problem, more compounds with m_0 close to that of $BaCu_2Si_2O_7$ are highly desirable.

Here, we report the synthesis, structure, and thermodynamic properties of (pipH)$CuBr_3$.[29] It is shown that (pipH)$CuBr_3$ is a weakly coupled HAFM spin-1/2 chain compound with $J \approx -17$ K and $J' = -0.91$ K. Below $T_N = 1.68$ K, the ordered magnetic moment of Cu(II) ions is $m_0 = 0.23\ \mu_B$, making (pipH)$CuBr_3$ another ideal compound to investigate the 1D−3D dimensional cross-over problem in magnetism.

■ EXPERIMENTAL SECTION

Synthesis. Single crystals of (pipH)$CuBr_3$ were synthesized by the evaporation method in a solution of ethanol. An 8.93 g (0.04 mol) amount of copper(II) bromide was dissolved in 225 mL of ethanol. A 2.93 mL amount of aqueous HBr (48% weight) was added to 1.98 mL of piperidine, resulting in 0.02 mol of piperidinium bromide (pipHBr). Then the solution of pipHBr was added slowly to the $CuBr_2$ solution. After 1 week of slow evaporation, black single crystals formed at the bottom of the beaker. The solution was decanted, and single crystals were harvested. The typical size of the crystals is 3 mm × 2 mm × 1.5 mm.

X-ray Diffraction. X-ray diffraction of a (pipH)$CuBr_3$ single crystal for structure determination was carried out on a Bruker SMART Apex (II) diffractometer (Mo Kα radiation, $\lambda = 0.71073$ Å). The crystal structure was solved by the direct method and refined via full-matrix least-squares techniques using the SHELXL-97 program package.[30] The results of cell parameters are listed in Table 1. Crystallographic data has been deposited at the Cambridge Crystallographic Data Center (CCDC 970073).

Thermodynamic Properties. The magnetic susceptibility of a (pipH)$CuBr_3$ single crystal as well as a powdered sample was measured by a MPMS SQUID magnetometer (Quantum Design). For the single crystal, magnetic fields were applied along the *b* axis and *c* axis and perpendicular to the *bc* plane, respectively. In the following, we define the direction perpendicular to the *bc* plane as the *a′* axis. Specific heat of (pipH)$CuBr_3$ single crystals was measured by the two-tau method in a small dilution refrigerator integrated to a Physical Property Measurement System (PPMS, Quantum Design) with magnetic fields applied along the *a′* and *c* axes.

■ RESULTS AND DISCUSSION

Table 1. Crystal Data and Structure Refinement for (pipH)$CuBr_3$

empirical formula	$C_5H_{12}NCuBr_3$
fw	389.43
temp.	296(2) K
wavelength	0.71073 Å
cryst syst	monoclinic
space group	*C*2/*c*
unit cell dimens	$a = 18.906(5)$ Å, $\alpha = 90°$
	$b = 8.834(3)$ Å, $\beta = 103.995(3)°$
	$c = 12.665(4)$ Å, $\gamma = 90°$
vol.	2052.6(10) Å^3
Z	8
calcd density	2.520 Mg/m^3
abs coeff	13.745 mm^{-1}
F(000)	1464
cryst size	0.3 × 0.2 × 0.15 mm
theta range for data collection	2.22−25.01°
limiting indices	$-21 \leq h \leq 22$
	$-9 \leq k \leq 10$
	$-14 \leq l \leq 15$
no. of reflns collected/unique	5645/1809 [$R_{int} = 0.0456$]
Completeness to $\theta = 25.01°$	99.7%
abs corr	semiempirical from equivalents
max and min transmission	0.7457 and 0.2959
refinement method	full-matrix least-squares on F^2
data/restraints/parameters	1809/0/92
goodness-of-fit on F^2	1.175
final *R* indices [$I > 2\sigma(I)$]	$R1 = 0.0296$, $wR2 = 0.0711$
R indices (all data)	$R1 = 0.0365$, $wR2 = 0.0811$
extinction coefficient	0.0081(3)
largest diff. peak and hole	0.916 and −0.580 e·Å^{-3}

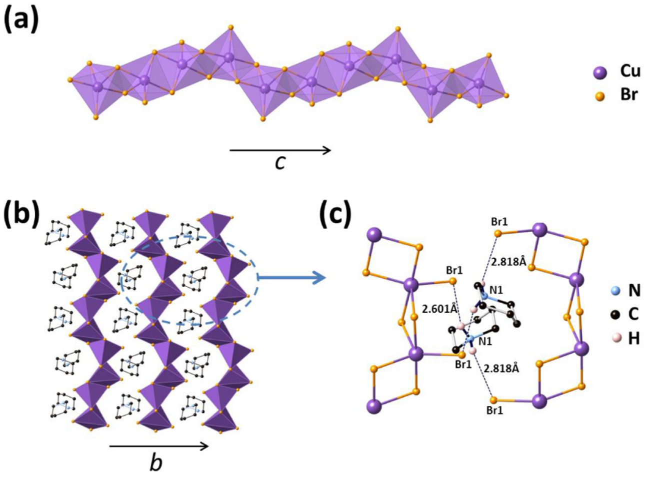

Figure 1. Crystal structure of (pipH)$CuBr_3$. (a) Illustration of a single zigzag chain of edge-sharing $CuBr_5$ units running along the *c* axis. (b) Packing diagram of the chains on the *bc* plane. Hydrogen atoms are omitted for clarity. (c) Details of the relative disposition of the piperidinium cations and their closest $CuBr_5$ pyramids. They are connected by hydrogen bonds, as illustrated by the dashed lines.

The compound (pipH)$CuBr_3$ crystallizes in the monoclinic space group *C*2/*c* with lattice parameters $a = 18.906(5)$ Å, $b = 8.834(3)$ Å, $c = 12.665(4)$ Å, and $\beta = 103.995(3)°$. Figure 1a shows the edge-sharing $CuBr_5$ units linking to form zigzag chains along the *c* axis with four inequivalent Cu(II) sites in each chain unit. In the square-pyramidal $CuBr_5$ unit, the Cu(II) ion is five coordinated. The axial bond is 2.8022 Å, and the basal bonds range from 2.4119 to 2.4628 Å. Neighboring Cu(II) ions with spin-1/2 along the chain are bridged by dibromide ions. This kind of dihalide-bridged magnetic chain with a five-coordinated Cu(II) ion can also be found in cyclopentylammonium trichlorocuprate(II), cyclohexylammonium trichlorocuprate(II), *n*-methyl-2-aminopyridiniumtrichlorocuprate(II) ($n = 4, 6$),[31] and [$NO_2BzMePy$][$CuCl_3$].[20,32] Among these five-coordinate halides, four serve as bridging ligands and the fifth as a terminal one. Along the *b* direction, chains are linked by hydrogen bonds, as shown in Figure 1b. In Figure 1c, we show the details of the relative deposition of the piperidinium cations and their closest $CuBr_5$ pyramids. They are connected by hydrogen bonds, as illustrated by the dashed lines. The chains are well isolated by the piperidinium cations and show ABA stacking order along the *a*′ direction. Crystal data is listed in Table 1.

The 1D magnetism of (pipH)$CuBr_3$ has been confirmed by magnetic susceptibility and specific heat measurements, as will be presented below. The magnetic susceptibility of (pipH)$CuBr_3$ powder was measured from 1.8 to 150 K in an applied field of 1000 Oe, and the results are shown in Figure 2a. The powder was obtained by grinding single crystals. The data show the characteristic feature of thr HAFM spin-1/2 chain with a broad maximum at about 10 K and a nonzero extrapolation value down to zero temperature,[33] as shown in the inset of Figure 2a. The susceptibility data from 4 to 150 K can be well fitted by the Bonner−Fisher formula for HAFM spin-1/2 chain.[34] The line in Figure 2a is the best fit with intrachain exchange interaction $J = -17.37 \pm 0.01$ K and Lander factor $g = 2.07$. The magnetic susceptibility of a (pipH)$CuBr_3$ single crystal with a field of 1000 Oe applied along the *a*′, *b*, and *c* axes is shown in Figure 2b. Again, all three curves can be fitted by the Bonner−Fisher formula from 4 to 150 K, and we get the parameters $J_{a'} = -17.16 \pm 0.02$ K, $g_{a'} = 2.32$, $J_b = -17.33 \pm 0.01$ K, $g_b = 2.00$, and $J_c = -16.64 \pm 0.02$ K, $g_c = 2.00$. Therefore, the magnetic susceptibility behavior strongly suggests that (pipH)$CuBr_3$ is a highly isotropic 1D HAFM spin-1/2 system.

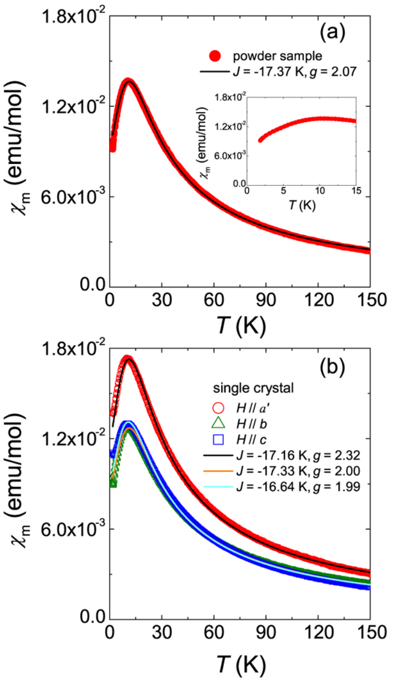

Figure 2. Magnetic susceptibility of (pipH)$CuBr_3$ as a function of temperature. (a) Data of powder sample. The line is fitting by the Bonner−Fisher formula for data from 4 to 150 K. (Inset) Susceptibility curve below 15 K which has a broad maximum around 10 K and a nonzero extrapolation value to zero temperature. (b) Data of a single crystal with fields applied along the *a*′ (red circle), *b* (olive triangle), and *c* (blue square) axes. Each curve is fitted by the Bonner−Fisher formula for data from 4 to 150 K. Fitting parameters are listed in the figure and text.

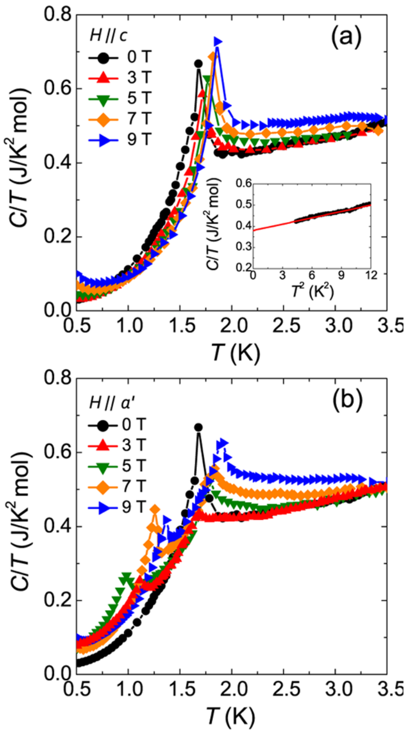

Figure 3. Low-temperature specific heat of (pipH)$CuBr_3$ single crystal. (a) Specific heat with fields applied along the *c* axis. (Inset) Zero-field specific heat from 2 to 3.5 K in which *C*/*T* is plotted as a function of T^2. The solid line is the fitting curve $C/T = 0.38 + 0.01T^2$. (b) Specific heat with fields applied along the *a*′ axis.

The specific heat of (pipH)$CuBr_3$ single crystals from 0.5 to 3.5 K is shown in Figure 3. The zero-field data from 2 to 3.5 K can be fitted by the equation

$$\frac{C}{T} = A + BT^2 \tag{1}$$

as seen in the inset of Figure 3a in which *C*/*T* is plotted as a function of T^2. The first term represents the 1D spinon contribution, and the second term is the phonon contribution. The fitting parameters are $A = 0.38$ J/K^2 mol and $B = 0.01$ J/K^4 mol. Theoretically, the specific heat contributed by spinons of the HAFM spin-1/2 chain can be calculated from the equation[34]

$$C_S = \frac{2Nk_B{}^2}{3J}T \tag{2}$$

where *N* is Avogadro's constant and k_B is the Boltzmann constant. Taking $J = -17.37$ K, the above equation gives the linear specific heat coefficient 0.32 J/K^2 mol, which is close to our experimental value of 0.38 J/K^2 mol. In this sense, the specific heat result further confirms the 1D magnetism in (pipH)$CuBr_3$. The linear specific heat contribution of spinons has also been observed in other HAFM spin-1/2 chain systems such as copper benzoate,[35] copper pyrimidine,[23] and copper pyrazine dinitrate.[24]

At zero field, *C*(*T*) shows a sharp peak at *T* = 1.68 K, suggesting the onset of a 3D ordered state. The transition temperature T_N varies with the strength and directions of the applied fields. For fields applied along the *c* axis, the ordering temperature T_N increases slightly with increasing field, as shown in Figure 3a. More interestingly, when the field is applied along the *a*′ axis, two peaks are clearly observed for $\mu_0H \geq 3$ T, indicating two successive magnetic phase transitions, as shown in Figure 3b. For $\mu_0H < 3$ T, the second low-temperature peak cannot be observed. We plot a rough μ_0H-T

phase diagram of (pipH)$CuBr_3$ in Figure 4. Data points correspond to the peaks of the specific heat curves in Figure 3, marked as T_{N1}, T_{N2}, and T_{N3}. The field can easily modulate the magnetic phase, which indicates that the Zeeman term $H_z = g\mu_B H \Sigma_i S_i^Z$ is important in the spin Hamiltonian

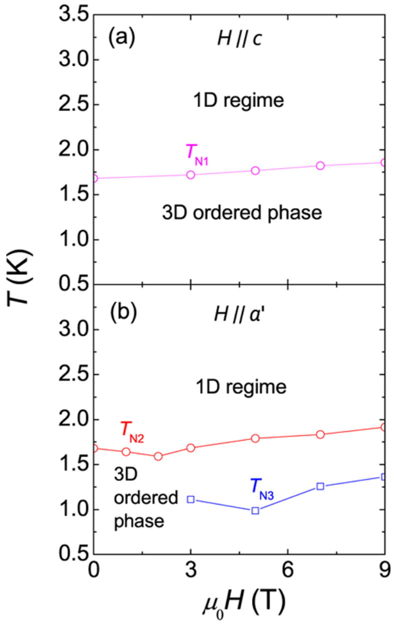

Figure 4. μ_0H-T phase diagram of (pipH)$CuBr_3$ derived from the specific heat measurement. Data points correspond to the peaks of the specific heat curves in Figure 3. For fields applied along the a' axis, two phase transitions are observed for $\mu_0H \geq 3$ T, as shown in the lower panel (b). However, the phase transition indicated by T_{N3} is not observed for $\mu_0H < 3$ T.

$$H_S = \sum_i \{-J\mathbf{S}_i\cdot\mathbf{S}_{i+1} - J' \sum_{\delta_\perp} \mathbf{S}_i\cdot\mathbf{S}_{i,\delta_\perp} + g\mu_B H S_i^Z\} \quad (3)$$

This is reasonable since the Zeeman energy is comparable with the exchange energy in our field range. The phenomenon of field-induced successive magnetic phase transitions has previously been observed in quantum antiferromagnets such as Cs_2CuCl_4,[36] which was attributed to competition between exchange interactions, Zeeman energy, quantum fluctuations, and Dzyaloshinsky−Moriya (D−M) interaction.[36] In (pipH)-$CuBr_3$, the D−M interaction should also be present since there is no inversion center between neighboring magnetic sites.[37] Each chain unit of (pipH)$CuBr_3$ has four inequivalent Cu(II) ions, and this alternating structure would induce staggered D−M interaction because of the different magnetic environment of neighboring Cu(II) sites. Since we cannot determine the magnetic structures in zero and magnetic fields, the exact magnetic phase diagram of (pipH)$CuBr_3$ needs to be revealed by other experiments such as neutron scattering measurement.

The 3D ordered state of weakly coupled HAFM spin-1/2 chains is rather exotic in which low-energy spin waves coexist with a high-energy multispinon continuum. From the ordering temperature T_N, we calculate the interchain exchange interaction J' by the empirical formula based on the quantum Monte Carlo (QMC) simulation[38−40]

$$|J'| = \frac{T_N}{0.932\sqrt{\ln\left(\frac{2.6|J|}{T_N}\right) + 0.5\ln\ln\left(\frac{2.6|J|}{T_N}\right)}} \quad (4)$$

and the ordered moment m_0 by the mean field theory[11]

$$m_0 = 1.017\sqrt{\frac{J'}{J}} \quad (5)$$

Taking $T_N = 1.68$ K at zero field and $J = -17.37$ K, the above equations give $J' = -0.91$ K and $m_0 = 0.23\ \mu_B$. This value of m_0 in the ordered state indicates 77% reduction from the saturated moment 1 μ_B of Cu(II) ions due to quantum fluctuations.

Experimentally, a weakly coupled HAFM spin-1/2 chain system suitable to study the 1D−3D dimensional cross-over problem should have a proper m_0 value. If m_0 is too small, as in Sr_2CuO_3 (~0.06 μ_B) and Ca_2CuO_3 (~0.09 μ_B),[27] the 1D character still dominates below the 3D ordered temperature and spin waves are hard to identify in the spectrum.[8,27] On the other hand, if m_0 is large, as in $KCuF_3$ (~0.54 μ_B),[26] the spin waves are very intense and the multispinon continuum is hard to isolate.[8,41] Thus far, $BaCu_2Si_2O_7$ with $m_0 = 0.16\ \mu_B$ is an ideal compound,[16] in which both spin waves and multispinon continuum have been clearly observed by inelastic neutron scattering measurements.[8] However, the experimentally obtained excitation spectrum of $BaCu_2Si_2O_7$ has serious discrepancies with theories on issues such as the dynamic structure factors of the novel longitudinal spin wave mode.[9,14] The m_0 of (pipH)$CuBr_3$ is close to that of $BaCu_2Si_2O_7$. Further studying the excitation spectrum of (pipH)$CuBr_3$ may help to resolve the 1D−3D dimensional cross-over problem in magnetism.

■ CONCLUSIONS

In summary, we report the synthesis, structure, and thermodynamic properties of a new quantum 1D magnetic compound (pipH)$CuBr_3$. The crystal shows 1D structure of Cu(II) ions connected by a dibromide bridge along the c axis. From the magnetic susceptibility and specific heat measurements, we demonstrate that (pipH)$CuBr_3$ can be well described by weakly coupled HAFM spin-1/2 chains with intrachain interaction $J \approx -17$ K and interchain interaction $J' = -0.91$ K. The proper value of $m_0 = 0.23\ \mu_B$ in the 3D ordered state at zero field makes it another ideal compound to study the 1D−3D dimensional cross-over problem in magnetism, besides $BaCu_2Si_2O_7$ with $m_0 = 0.16\ \mu_B$. The observation of two successive magnetic transitions in specific heat measurements indicates a complex magnetic phase diagram of (pipH)$CuBr_3$, which is roughly constructed.

■ ASSOCIATED CONTENT

Ⓢ Supporting Information

Crystallographic data in CIF format, tables of atomic coordination, and selected bond lengths and angles.

This material is available free of charge via the Internet at http://pubs.acs.org.

■ AUTHOR INFORMATION

Corresponding Authors

*E-mail: zhanglijuan@fudan.edu.cn.
*E-mail: shiyan_li@fudan.edu.cn.

Notes

The authors declare no competing financial interest.

■ ACKNOWLEDGMENTS

We thank Yan Chen (Fudan Univerisity) for helpful discussions. This work was supported by the Natural Science Foundation of China, the Ministry of Science and Technology of China (National Basic Research Program No. 2012CB821402), and the Program for Professor of Special Appointment (Eastern Scholar) at Shanghai Institutions of Higher Learning.

■ REFERENCES

(1) Majlis, N. *The quantum theory of magnetism*, 2nd ed.; World Scientific Publishing Co. Pte. Ltd.: Singapore, 2007.

(2) Bethe, H. A. *Z. Phys.* **1931**, *71*, 205−226.

(3) Huthén, L. *Ark, Mat., Astron. Fys.* **1938**, *26A*, No. 11.

(4) Tennant, D. A.; Cowley, R. A.; Nagler, S. E.; Tsvelik, A. M. *Phys. Rev. B* **1995**, *52*, 13368−13380.

(5) Coldea, R.; Tennant, D. A.; Tsvelik, A. M.; Tylczynski, Z. *Phys. Rev. Lett.* **2001**, *86*, 1335−1338.

(6) Coldea, R.; Tennant, D. A.; Tylczynski, Z. *Phys. Rev. B* **2003**, *68*, 134424.

(7) Kohno, M.; Starykh, O. A.; Balents, L. *Nat. Phys.* **2007**, *3*, 790−795.

(8) Zheludev, A.; Kenzelmann, M.; Raymond, S.; Ressouche, E.; Masuda, T.; Kakurai, K.; Maslov, S.; Tsukada, I.; Uchinokura, K.; Wildes, A. *Phys. Rev. Lett.* **2000**, *85*, 4799−4802.

(9) Zheludev, A.; Kakurai, K.; Masuda, T.; Uchinokura, K.; Nakajima, K. *Phys. Rev. Lett.* **2002**, *89*, 197205.

(10) Lake, B.; Tennant, D. A.; Nagler, S. E. *Phys. Rev. B* **2005**, *71*, 134412.

(11) Schulz, H. J. *Phys. Rev. Lett.* **1996**, *77*, 2790−2793.

(12) Essler, F. H. L.; Tsvelik, A. M.; Delfino, G. *Phys. Rev. Lett.* **1997**, *56*, 11001−11013.

(13) Lake, B.; Tennant, D. A.; Nagler, S. E. *Phys. Rev. Lett.* **2000**, *85*, 832−835.

(14) Zheludev, A.; Raymond, S.; Regnault, L.-P.; Essler, F. H. L.; Kakurai, K.; Masuda, T.; Uchinokura, K. *Phys. Rev. B* **2003**, *67*, 134406.

(15) Kenzelmann, M.; Zheludev, A.; Raymond, S.; Ressouche, E.; Masud, T.; Böni, P.; Kakurai, K.; Tsukada, I.; Uchinokura, K.; Coldea, R. *Phys. Rev. B* **2001**, *64*, 054422.

(16) Tsukada, I.; Sasago, Y.; Uchinokura, K.; Zheludev, A.; Maslov, S.; Shirane, G.; Kakurai, K.; Ressouche, E. *Phys. Rev. B* **1999**, *60*, 6601−6607.

(17) Motoyama, N.; Eisaki, H.; Uchida, S. *Phys. Rev. Lett.* **1996**, *76*, 3212−3215.

(18) Kiryukhin, V.; Kim, Y. J.; Thomas, K. J.; Chou, F. C.; Erwin, R. W.; Huang, Q.; Kastner, M. A.; Birgeneau, R. J. *Phys. Rev. B* **2001**, *63*, 144418.

(19) Hirakawa, K.; Kurogi, Y. *Suppl. Prog. Theor. Phys.* **1970**, *46*, 147−161.

(20) Landee, C. P.; Turnbull, M. M. *Eur. J. Inorg. Chem.* **2013**, 2266−2285.

(21) Date, M.; Yamazaki, H.; Motokawa, M.; Tazawa, S. *Suppl. Prog. Theor. Phys.* **1970**, *46*, 194−209.

(22) Ishida, T.; Nakayama, K.; Nakagawa, M.; Sato, W.; Ishikawa, Y.; Yasui, M.; Iwasaki, F.; Nogami, T. *Synth. Met.* **1997**, *85*, 1655−1658.

(23) Feyerherm, R.; Abens, S.; Günther, D.; Ishida, T.; Meiβner, M.; Meschke, M.; Nogami, T.; Steiner, M. *J. Phys.: Condens. Matter* **2000**, *12*, 8495−8509.

(24) Hammar, P. R.; Stone, M. B.; Reich, D. H. *Phys. Rev. B* **1999**, *59*, 1008−1015.

(25) Chen, Y.; Stone, M. B.; Kenzelmann, M.; Batista, C. D.; Reich, D. H.; Broholm, C. *Phys. Rev. B* **2007**, *75*, 214409.

(26) Hutchings, M. T.; Samuelsen, E. J.; Shirane, G.; Hirakawa, K. *Phys. Rev.* **1969**, *188*, 919−923.

(27) Kojima, K. M.; Fudamoto, Y.; Larkin, M.; Luke, G. M.; Merrin, J.; Nachumi, B.; Uemura, Y. J.; Motoyama, N.; Eisaki, H.; Uchida, S.; Yamada, K.; Endoh, Y.; Hosoya, S.; Sternlieb, B. J.; Shirane, G. *Phys. Rev. Lett.* **1997**, *78*, 1787−1790.

(28) Casola, F.; Shiroka, T.; Glazkov, V.; Feiguin, A.; Dhalenne, G.; Revcolevschi, A.; Zheludev, A.; Ott, H.-R.; Mesot, J. *Phys. Rev. B* **2012**, *86*, 165111.

(29) In previous literature onspin ladder compound $(\mathrm{pipH})_2\mathrm{CuBr}_4$ (Patyal, B. R.; Scott, B. L.; Willett, R. D. *Phys. Rev. B* **1990**, *41*, 1657−1663), the authors also mentioned the produce of $(\mathrm{pipH})\mathrm{CuBr}_3$, but no structure information or properties of this compound were reported..

(30) Sheldrick, G. M. *Acta Crystallogr., Sect. A* **2008**, *64*, 112−122.

(31) Geiser, U.; Gaura, R. M.; Willett, R. D.; West, D. X. *Inorg. Chem.* **1986**, *25*, 4203−4212.

(32) Han, S.; Liu, X. Y.; Cai, Z. F.; Wu, Z. P.; Yin, W. T.; Xie, X. D.; Zhou, J. R.; Yang, L. M.; Ni, C. L. *Inorg. Chem. Commun.* **2012**, *24*, 91−94.

(33) Dagotto, E.; Rice, T. M. *Science* **1996**, *271*, 618−623.

(34) Bonner, J. C.; Fisher, M. E. *Phys. Rev.* **1964**, *135*, A640−A658.

(35) Dender, D. C.; Hammar, P. R.; Reich, D. H.; Broholm, C.; Aeppli, G. *Phys. Rev. B* **1997**, *79*, 1750−1753.

(36) Tokiwa, Y.; Radu, T.; Coldea, R.; Wilhelm, H.; Tylczynski, Z.; Steglich, F. *Phys. Rev. B* **2006**, *73*, 134414.

(37) Moriya, T. *Phys. Rev. B* **1960**, *120*, 91−98.

(38) Yasuda, C.; Todo, S.; Hukushima, K.; Alet, F.; Keller, M.; Troyer, M.; Takayama, H. *Phys. Rev. Lett.* **2005**, *94*, 217201.

(39) Lancaster, T.; Blundell, S. J.; Brooks, M. L.; Baker, P. J.; Pratt, F. L.; Manson, J. L.; Landee, C. P.; Baines, C. *Phys. Rev. B* **2006**, *73*, 020410.

(40) Blundella, S. J.; Lancastera, T.; Prattb, F. L.; Bakera, P. J.; Brooksa, M. L.; Bainesc, C.; Mansond, J. L.; Landeee, C. P. *J. Phys. Chem. Solids* **2007**, *68*, 2039−2043.

(41) Tennant, D. A.; Nagler, S. E.; Welz, D.; Shirane, G.; Yamada, K. *Phys. Rev. B* **1995**, *52*, 13381−13389.